Exchange of Two-Spin Order in Nuclear Magnetic Resonance: Separation of Exchange and Cross-Relaxation Processes

Gerhard Wagner,[†] Geoffrey Bodenhausen,[‡] Norbert Müller,[†,‡] Mark Rance,[†,‡,§] Ole W. Sørensen,[‡] Richard R. Ernst,[‡] and Kurt Wüthrich*[†]

Contribution from the Institut für Molekularbiologie und Biophysik, Eidgenössische Technische Hochschule, 8093 Zürich, Switzerland, and Laboratorium für Physikalische Chemie, Eidgenössische Technische Hochschule, 8092 Zürich, Switzerland. *Received April 22, 1985*

Abstract: The measurement of the migration of longitudinal two-spin order by two-dimensional (2D) exchange spectroscopy or by selective one-dimensional (1D) methods (2D or 1D "*zz*-exchange spectroscopy") allows one to differentiate unambiguously between chemical exchange and cross-relaxation processes in complex nuclear spin systems, provided a fragment with at least two coupled spins is transferred from one site to another in the exchange process. Compared to conventional 2D exchange spectroscopy, *zz*-exchange studies have the advantage that cross-peaks due to migration of *zz*-order usually suffer less from overlaps than the corresponding cross-peaks in 2D exchange spectra, which often appear close to the diagonal. An attractive feature of *zz*-exchange spectroscopy is that it allows one to distinguish cross-relaxation processes (nuclear Overhauser effects) that occur within scalar-coupling spin systems (e.g., within individual amino acid residues in proteins) from processes where magnetization is transferred between different spin systems (e.g., between different amino acid residues in proteins).

Nuclear magnetic resonance[1] provides unique means for measuring the rates of chemical exchange processes such as internal rotations, bond shifts, valence isomerization, etc., in systems which are in dynamic chemical equilibrium. This can be achieved by selective labeling (e.g., through selective inversion) of the magnetization of a spin which has a chemical shift characteristic of one of the sites and by monitoring the transfer of the nonequilibrium magnetization to the other sites.[2,3] The results of such experiments can, however, be ambiguous, since the transfer of magnetization may result either from migration of nuclei from one site to another through an exchange process or from a magnetic transfer through cross-relaxation, and a superposition of both mechanisms can often not be excluded a priori. For example, the interchange of the populations of two states $|\alpha\beta>$ and $|\beta\alpha>$ can be brought about by swapping the nuclei between the two sites or by a spin flip–flop process.

In systems with complex exchange networks, such as macromolecules and biopolymers in solution, the migration of labeled magnetization can be monitored by two-dimensional exchange spectroscopy, which has proven useful both for characterizing slow chemical exchange[4] and for measuring nuclear Overhauser effects.[5] The similarity between exchange and cross-relaxation is reflected in the normalized integrated amplitudes $a_{k,l}$ of cross- and diagonal-peaks with frequency coordinates $(\omega_1,\omega_2) = (\Omega_l,\Omega_k)$:

$$a_{k,l}(\tau_m) = [\exp\{\boldsymbol{L}\tau_m\}]_{kl} \simeq \delta_{kl} + (\boldsymbol{L})_{kl}\tau_m + \tfrac{1}{2}\Sigma_j(\boldsymbol{L})_{kj}(\boldsymbol{L})_{jl}\tau_m^2 + \ldots \quad (1)$$

where the dynamic matrix $\boldsymbol{L}$ contains contributions from both exchange and cross-relaxation rates:

$$\boldsymbol{L} = \boldsymbol{K} - \boldsymbol{R} \quad (2)$$

The elements K_{ij} of the kinetic matrix $\boldsymbol{K}$ represent first-order rate constants of chemical processes $[A_j] \rightarrow [A_i]$, and the off-diagonal elements R_{ij} of the relaxation matrix $\boldsymbol{R}$ represent cross-relaxation rate constants. The form of eq 1 and 2 clearly shows that conventional 2D exchange experiments (or, for that matter, equivalent 1D saturation transfer methods) can only lead to a determination of the matrix elements of $\boldsymbol{L}$. The contributions of $\boldsymbol{K}$ and $\boldsymbol{R}$ can be separated by studying the dependence of the rates $L_{ij} = K_{ij} - R_{ij}$ on the static magnetic field, which may affect R_{ij} but not K_{ij}. On the other hand, if one deals with an Arrhenius-type thermally activated process, a variation of the temperature has a more pronounced effect on K_{ij} than on R_{ij}, if it can be assumed that the correlation time τ_c changes little over the relevant temperature range.

We propose in this paper to distinguish different exchange and cross-relaxation processes by monitoring the transfer of the polarization associated with a *set* of spins. In cross-relaxation, the magnetic pair interactions lead to polarization transfer of individual spins, while chemical exchange processes may involve the simultaneous transfer of several magnetic nuclei. Multispin processes may be distinguished from one-spin processes by observing the transfer of longitudinal two-spin order (or of *p*-spin order if appropriate). Two or more spins can be "labeled" by creating a mutually ordered state which can be described by density operator terms of the type $2I_{kz}I_{lz}$, $4I_{kz}I_{lz}I_{mz}$, etc.[6,7] The transfer of this type of order from one set of spins to another indicates simultaneous exchange of all spins.

We exemplify this principle by considering systems where exchange and cross-relaxation occur simultaneously. The distinction of intra- and intermolecular chemical exchange processes will be discussed elsewhere.[8] Two-spin order also allows one to focus attention on cross-relaxation processes between spins that possess a common coupling partner within a network of scalar-coupled spins (e.g., within an amino acid residue or within the building blocks of nucleic acids). Cross-relaxation processes between spins that do not have a common coupling partner (e.g., between protons in different amino acid residues in a protein) cannot be observed by *zz*-exchange spectroscopy.

Two-Dimensional *zz*-Exchange Spectroscopy

To monitor the exchange of two-spin order, one may employ a simple variation[6] of the 2D exchange experiment, which we shall refer to as "*zz*-exchange spectroscopy". This experiment is based

[†] Institut für Molekularbiologie und Biophysik.
[‡] Laboratorium für Physikalische Chemie.
[§] Current address: Department of Molecular Biology, Research Institute, Scripps Clinic, 10666 North Torrey Pines Road, La Jolla, California 92037.

(1) Abbrevations used: NOE, nuclear Overhauser enhancement; NOESY, two-dimensional nuclear Overhauser spectroscopy; COSY, two-dimensional correlation spectroscopy; DQF-COSY, double-quantum filtered correlation spectroscopy; BPTI, basic pancreative trypsin inhibitor (Trasylol, Bayer AG, Leverkusen); TSP, sodium 3-trimethylsilyl-(2,2,3,3-$^2H_4$)-propionate; Tyr, tyrosine; Ile, isoleucine; Arg, arginine, Pro, proline.

(2) Forsén, S.; Hoffmann, R. A.: (a) *J. Chem. Phys.* **1963**, *39*, 2892–2801. (b) *J. Chem. Phys.* **1964**, *40*, 1189–1196. (c) *J. Chem. Phys.* **1966**, *45*, 2049–2060.
(3) (a) Jeener, J.; Meier, B. H.; Bachmann, P.; Ernst, R. R. *J. Chem. Phys.* **1979**, *71*, 4546–4553. (b) Macura, S.; Ernst, R. R. *Mol. Phys.* **1980**, *41*, 95–117.
(4) Meier, B. H.; Ernst, R. R. *J. Am. Chem. Soc.* **1979**, *101*, 6441–6442.
(5) Kumar, Anil; Ernst, R. R.; Wüthrich, K. *Biochem. Biophys. Res. Commun.* **1980**, *95*, 1–6.
(6) Bodenhausen, G.; Wagner, G.; Rance, M.; Sørensen, O. W.; Würthrich, K.; Ernst, R. R. *J. Magn. Reson.* **1984**, *59*, 542–550.
(7) Sørensen, O. W.; Eich, G. W.; Levitt, M. H.; Bodenhausen, G.; Ernst, R. R. *Prog. Nucl. Magn. Reson. Spectrosc.* **1983**, *16*, 16–192.
(8) Pastore, A.; Bodenhausen, G.; Sørensen, O. W.; Levitt, M. H.; Ernst, R. R. to be published.

0002-7863/85/1507-6440$01.50/0

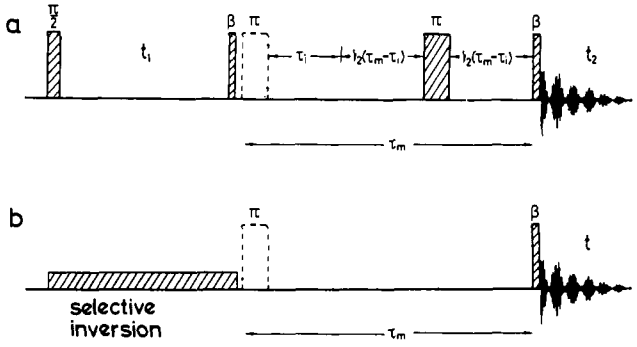

Figure 1. Schemes for the excitation and detection of longitudinal two-spin order (zz-order). (a) Two-dimensional zz-exchange spectroscopy. (b) One-dimensional version of the experiment. The flip angles of the pulses labeled with β are typically $\pi/4$. The nonselective π pulses drawn with broken lines are applied on alternate scans only. The hatched π pulse in (a) is applied in all scans and shifted within the τ_m period in order to suppress artifacts due to zero-quantum coherence (J peaks).

on the pulse sequence shown in Figure 1a, designed to monitor the creation, migration, and reconversion of longitudinal p-spin order of the type $2I_{kz}I_{lz}$, $4I_{kz}I_{lz}I_{mz}$, etc.[7] Figure 2a shows the population distribution associated with two-spin order in a two-spin system. This type of order does not involve a polarization of either spin and does not lead to a magnetic dipole moment but represents a mutually ordered state with a magnetic quadrupole character. It is instructive to compare two-spin order with Zeeman polarization I_{kz} shown in Figure 2b.

Two-spin order can migrate either by simultaneous exchange of both spins $2I_{kz}I_{lz} \rightarrow 2I_{mz}I_{nz}$ or by intramolecular exchange or cross-exchange of a single spin $I_l \rightarrow I_m$, leading to a conversion of two-spin order $2I_{kz}I_{lz} \rightarrow 2I_{kz}I_{mz}$. Such processes can only be observed if the ordered spins are mutually coupled, i.e., one must have $J_{kl} \neq 0$ and $J_{mn} \neq 0$ to monitor the simultaneous exchange of two spins and $J_{kl} \neq 0$ and $J_{km} \neq 0$ to observe the migration of a single spin $I_l \rightarrow I_m$. These restrictions make it possible to distinguish various dynamic processes as discussed below.

The extension to the transfer of p-spin order with $p > 2$ is straightforward. Thus the migration of a term $4I_{kz}I_{lz}I_{mz}$ would allow one to investigate exchange processes where a fragment containing three coupled spins is transferred from one site to another.

In the pulse sequence for zz-exchange spectroscopy, shown in Figure 1a, longitudinal spin order is excited at the beginning of the mixing interval τ_m by converting antiphase single quantum coherence by applying a radio frequency pulse with a flip angle $\beta \neq \pi/2$ (typically $\beta = \pi/4$). This pulse acts on antiphase terms such as $2I_{kx}I_{lz}$ and $4I_{kx}I_{lz}I_{mz}$, etc., which appear at the end of the evolution period if the spin system features resolved couplings. The generation of longitudinal spin order under the propagator $\exp\{-i\beta F_y\}$ of a nonselective radio frequency pulse with rotation angle β applied along the y axis of the rotating frame is described by[7]

$$2I_{kx}I_{lz} \xrightarrow{\beta(I_{ky}+I_{ly})} -2I_{kz}I_{lz}\cos\beta\sin\beta + \text{other terms} \quad (3)$$

$$4I_{kx}I_{lz}I_{mz} \xrightarrow{\beta(I_{ky}+I_{ly}+I_{my})} -4I_{kz}I_{lz}I_{mz}\cos^2\beta\sin\beta + \text{other terms} \quad (4)$$

The terms generated in eq 3 and 4 are referred to as longitudinal two- and three-spin order, respectively.

In the mixing interval, p-spin order can migrate due to exchange or cross-relaxation. In macromolecules in the slow motion limit ($\omega_0\tau_c \gg 1$), relaxation processes involving single and double quantum transition probabilities W_1 and W_2 (e.g., processes $|\alpha\rangle \rightarrow |\beta\rangle$ and $|\alpha\alpha\rangle \rightarrow |\beta\beta\rangle$) can be neglected on the time scale of τ_m, and cross-relaxation is dominated by processes $|\alpha\beta\rangle \rightarrow |\beta\alpha\rangle$ associated with the zero-quantum transition probability W_0. In this limit, the order is conserved, e.g., two-spin order can only be transformed into other forms of two-spin order. The amplitudes of these transformation processes can be expressed with τ_m-dependent coefficients, which are labeled by generalizing the indices of eq 1:

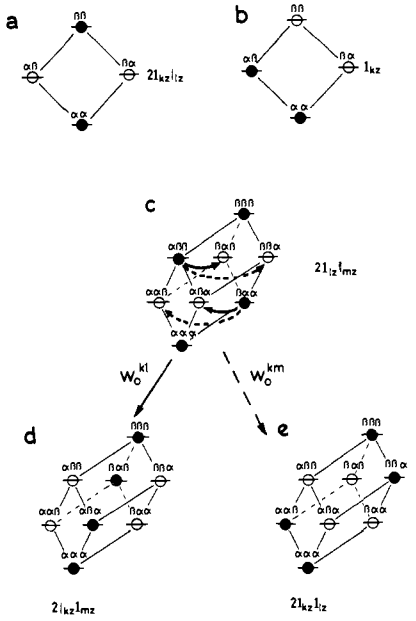

Figure 2. (a) Distribution of populations for two-spin order $2I_{kz}I_{lz}$ in a two-spin system. Filled and open symbols represent populations that are greater or smaller than in a state where all populations are equal. (b) Distribution corresponding to Zeeman order (polarization) I_{kz}. (c) Populations corresponding to two-spin order $2I_{lz}I_{mz}$ in a three-spin system. The states are labeled in the order M_{kz}, M_{lz}, and M_{mz}. Through zero-quantum relaxation W_0^{kl} (flip–flop process of spins I_k and I_l, solid arrows), the populations migrate and lead to a partial transformation of $2I_{lz}I_{mz}$ into $2I_{kz}I_{mz}$, resulting in the population distribution (d). Through W_0^{km} relaxation (flip–flop of spins I_k and I_m, dashed arrows), one obtains a partial transformation of $2I_{lz}I_{mz}$ into $2I_{kz}I_{lz}$, resulting in the population distribution (e).

$$2I_{kz}I_{lz} \rightarrow a_{kl,kl}(\tau_m)2I_{kz}I_{lz} + a_{km,kl}(\tau_m)2I_{kz}I_{mz} + a_{ml,kl}(\tau_m)2I_{mz}I_{lz} + a_{mn,kl}(\tau_m)2I_{mz}I_{nz} \quad (5)$$

$$4I_{kz}I_{lz}I_{mz} \rightarrow a_{klm,klm}(\tau_m)4I_{kz}I_{lz}I_{mz} + a_{kln,klm}(\tau_m)4I_{kz}I_{lz}I_{nz} + \text{other terms} \quad (6)$$

If relaxation processes W_1 and W_2 cannot be neglected, it is possible to observe a change from one order to another, for example

$$2I_{kz}I_{lz} \rightarrow a_{k,kl}(\tau_m)I_{kz} + a_{l,kl}(\tau_m)I_{lz} + a_{klm,kl}(\tau_m)I_{kz}I_{lz}I_{mz} + \text{other terms} \quad (7)$$

We may note in parentheses that the migration of one-spin order terms, such as

$$I_{kz} \rightarrow a_{k,k}(\tau_m)I_{kz} + a_{l,k}(\tau_m)I_{lz} \quad (8)$$

is responsible for diagonal and cross-peaks in normal 2D Overhauser spectroscopy (NOESY) with amplitudes given by eq 1.

At the end of the mixing interval, p-spin order is partially reconverted into observable single quantum coherence:

$$2I_{kz}I_{lz} \xrightarrow{\beta(I_{ky}+I_{ly})} (2I_{kx}I_{lz} + 2I_{kz}I_{lx})\cos\beta\sin\beta + \text{nonobservable terms} \quad (9)$$

$$4I_{kz}I_{lz}I_{mz} \xrightarrow{\beta(I_{ky}+I_{ly}+I_{my})} (4I_{kx}I_{lz}I_{mz} + 4I_{kz}I_{lx}I_{mz} + 4I_{kz}I_{lz}I_{mx})\cos^2\beta\sin\beta + \text{nonobservable terms} \quad (10)$$

Clearly, the experiment of Figure 1a is closely related to conventional 2D exchange spectroscopy but uses two pulses $0 < \beta < \pi/2$ to excite and reconvert scalar order, in analogy to the Jeener–Broeckaert experiment.[9] Typically, both pulses have flip

(9) Jeener, J.; Broeckaert, P. *Phys. Rev.* **1967**, *157*, 232–240.

angles $\beta = \pi/4$, as opposed to $\beta = \pi/2$ in conventional 2D exchange or 2D Overhauser spectroscopy. In addition, a π pulse is inserted at the beginning of the mixing period in every second scan, and the signals are stored separately. Linear combinations of these signals allow one to separate terms with even and odd numbers of I_{kz} operators at the beginning of the τ_m interval: the sum gives spectra associated with even-ordered terms (two- and four-spin order, etc.), and the difference yields only signal contributions from terms of odd orders (one- and three-spin order, etc.). To discriminate against processes where the order is changed in the course of τ_m as in eq 7, one may insert another π pulse at the end of the mixing period in alternate experiments and make suitable linear combinations of signals obtained from four different experiments with and without π pulses at the beginning or end of τ_m.

The insertion of a π pulse in alternate scans not only selects zz-components but also retains the x components of double and zero-quantum coherence:

$$\{2QT\}_x = \tfrac{1}{2}(2I_{kx}I_{lx} - 2I_{ky}I_{ly}) \quad (11)$$

$$\{ZQT\}_x = \tfrac{1}{2}(2I_{kx}I_{lx} + 2I_{ky}I_{ly}) \quad (12)$$

Double quantum coherence can be eliminated by phase-cycling,[10,11] and zero-quantum coherence may be suppressed by inserting another π pulse at variable points in the mixing interval τ_m.[10,12,13]

Migration of Two-Spin Order through Cross-Relaxation in Three-Spin Systems

Consider a system with three weakly coupled spins I_k, I_l, and I_m. Figure 2c shows how two-spin order $2I_{lz}I_{mz}$ can be represented in terms of populations of the eigenstates. The migration of the populations is governed by the master equation

$$\frac{d}{dt}\Delta\mathbf{P} = \boldsymbol{W}\Delta\mathbf{P} = \boldsymbol{W}[\mathbf{P}(t) - \mathbf{P}(eq)] \quad (13)$$

where $\mathbf{P}(t)$ and $\mathbf{P}(eq)$ denote population vectors at time t and at equilibrium, and where $\boldsymbol{W}$ is the relaxation matrix. For simplicity, we restrict the discussion to systems with slow rotational diffusion (macromolecules) with long correlation times, i.e., $\omega_0\tau_c \gg 1$. In this case, only zero-quantum transition probabilities W_0 need to be considered, since single- and double-quantum relaxation pathways described by the transition probabilities W_1 and W_2 can be neglected on the time scale of τ_m. With reference to the numbering of the eigenstates in Figure 2, one obtains a simplified relaxation matrix, eq 14, where $\Delta P_{\alpha\beta\alpha}$, for example, indicates the

$$\frac{d}{dt}\begin{vmatrix}\Delta P_{\alpha\alpha\alpha}\\ \Delta P_{\alpha\alpha\beta}\\ \Delta P_{\alpha\beta\alpha}\\ \Delta P_{\beta\alpha\alpha}\\ \Delta P_{\alpha\beta\beta}\\ \Delta P_{\beta\alpha\beta}\\ \Delta P_{\beta\beta\alpha}\\ \Delta P_{\beta\beta\beta}\end{vmatrix} = \begin{vmatrix} D_{11} & & & & & & & \\ & D_{22} & W_0^{lm} & W_0^{km} & & & & \\ & W_0^{lm} & D_{33} & W_0^{kl} & & & & \\ & W_0^{km} & W_0^{kl} & D_{44} & & & & \\ & & & & D_{55} & W_0^{kl} & W_0^{km} & \\ & & & & W_0^{kl} & D_{66} & W_0^{lm} & \\ & & & & W_0^{km} & W_0^{lm} & D_{77} & \\ & & & & & & & D_{88}\end{vmatrix} \begin{vmatrix}\Delta P_{\alpha\alpha\alpha}\\ \Delta P_{\alpha\alpha\beta}\\ \Delta P_{\alpha\beta\alpha}\\ \Delta P_{\beta\alpha\alpha}\\ \Delta P_{\alpha\beta\beta}\\ \Delta P_{\beta\alpha\beta}\\ \Delta P_{\beta\beta\alpha}\\ \Delta P_{\beta\beta\beta}\end{vmatrix} \quad (14)$$

deviation from thermal equilibrium of the population of the state $|\alpha\beta\alpha\rangle = |M_{kz} = +^1/_2, M_{lz} = -^1/_2, M_{mz} = +^1/_2\rangle$, and where the diagonal elements are given by $D_{ii} = -\sum_{i\neq j}W_{ij}$ (note that $D_{11} = D_{88} = 0$). The zero quantum transition probability W_0^{kl} refers to a flip–flop process involving spins k and l, for example, $|\alpha\beta\gamma\rangle \rightarrow |\beta\alpha\gamma\rangle$, where the polarization $\gamma = \alpha$ or β of the third spin I_m is immaterial. Because the single and double quantum transition probabilities W_1 and W_2 have been neglected in eq 14, only

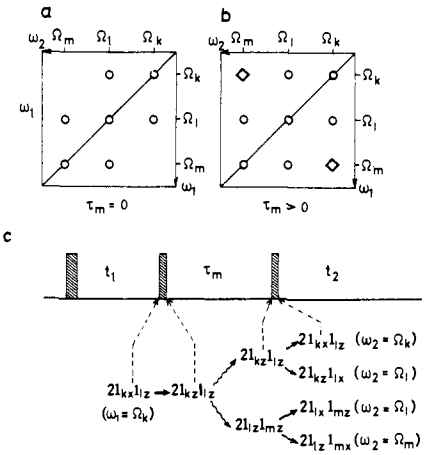

Figure 3. Schematic zz-spectra of a linear three-spin system with $J_{km} = 0$: (a) for short mixing times ($W_0^{kl}\tau_m$, $W_0^{km}\tau_m$, $W_0^{lm}\tau_m \ll 1$), where the appearance is similar to that of a double-quantum-filtered correlation spectrum (DQF-COSY),[14-16] with antiphase multiplets represented by circles; (b) for a longer mixing time, with partial migration of zz-order, leading to additional cross-peaks indicated by diamonds. (c) "Genealogical tree" showing the offspring of one of the antiphase magnetization terms that occur at the end of the evolution period. These terms contribute to multiplets with frequency coordinates that correspond to the chemical shifts of the nuclei that appear with transverse operator terms in the evolution and detection periods.

populations of states with the same total magnetic quantum number $M_i = -^3/_2, -^1/_2, ^1/_2$, or $^3/_2$ can exchange, hence the block structure of the $\boldsymbol{W}$ matrix.

The resulting population distribution can be expressed as linear combination of the base operators $\{\mathbf{1}, I_{kz}, I_{lz}, I_{mz}, 2I_{kz}I_{lz}, \ldots, 4I_{kz}I_{lz}I_{mz}\}$. The restriction to W_0 pathways implies that there are no cross-terms between different orders, i.e., there are no processes of the type described by eq 7. In a three-spin system, the initial rate solution of the master equation can be described by eq 5 with the coefficients:

$$a_{kl,kl}(\tau_m) = 1 - (W_0^{lm} + W_0^{km})\tau_m$$

$$a_{km,kl}(\tau_m) = W_0^{lm}\tau_m$$

$$a_{lm,kl}(\tau_m) = W_0^{km}\tau_m \quad (15)$$

The resulting zz-exchange spectrum in a three-spin system with a vanishing coupling $J_{km} = 0$ is shown schematically in Figure 3. In the absence of cross-relaxation ($W_0\tau_m \ll 1$), the cross- and diagonal-peaks are fully analogous to those obtained in double-quantum-filtered correlation spectroscopy.[14-16] If one selects a suitable phase-cycling scheme,[11] all multiplet components have pure 2D absorption peak-shapes with alternating signs, and the appearance of cross-peaks depends only on the existence of a nonvanishing coupling J_{kl}. For clarity, it has been asumed in Figure 3 that $J_{km} = 0$, so that it is not possible to excite or reconvert a term $2I_{kz}I_{mz}$, and in the absence of cross-relaxation there are no cross-peaks of $(\omega_1,\omega_2) = (\Omega_k,\Omega_m)$ and (Ω_m,Ω_k). However, cross-peaks make their appearance at these frequency coordinates if cross-relaxation leads to a transfer $2I_{kz}I_{lz} \rightarrow 2I_{lz}I_{mz}$ and $2I_{lz}I_{mz} \rightarrow 2I_{kz}I_{lz}$, respectively. The "genealogical tree" of operator terms shown in Figure 3 leads to four terms that contribute to three multiplets in a row with $\omega_1 = \Omega_k$. In this three-spin system, there are four such families, starting with $2I_{kx}I_{lz}$, $2I_{kz}I_{lx}$, $2I_{lx}I_{mz}$ and $2I_{lz}I_{mx}$, whose "offspring" of 16 operator terms contributes to the nine multiplets in Figure 3b.

If $J_{km} = 0$, the intensity of the cross-peak at $(\omega_1,\omega_2) = (\Omega_k,\Omega_m)$ is directly proportional to $a_{lm,kl} = W_0^{km}\tau_m$, provided the initial

(10) Macura, S.; Huang, Y.; Suter, D.; Ernst, R. R. *J. Magn. Reson.* **1981**, *43*, 259–281.
(11) Bodenhausen, G.; Kogler, H.; Ernst, R. R. *J. Magn. Reson.* **1984**, *58*, 370–388.
(12) Macura, S.; Wüthrich, K.; Ernst, R. R. *J. Magn. Reson.* **1982**, *46*, 269–282.
(13) Rance, M.; Bodenhausen, G.; Wagner, G.; Wüthrich, K.; Ernst, R. R. *J. Magn. Reson.* **1985**, *62*, 497–510.
(14) Piantini, U.; Sørensen, O. W.; Ernst, R. R. *J. Am. Chem. Soc.* **1982**, *104*, 6800–6801.
(15) Shaka, A. J.; Freeman, R. *J. Magn. Reson.* **1984**, *15*, 169–173.
(16) Rance, M.; Sørensen, O. W.; Bodenhausen, G.; Wagner, G.; Ernst, R. R.; Wüthrich, K. *Biochem. Biophys. Res. Commun.* **1983**, *117*, 479–485.

rate approximation is fulfilled. This amplitude is equivalent to the intensity of the corresponing cross-peak at $(\omega_1,\omega_2) = (\Omega_k,\Omega_m)$ in a conventional 2D exchange spectrum, where the migration $I_{kz} \rightarrow I_{mz}$ is associated with the amplitude $a_{m,k}(\tau_m) = W_0^{km}\tau_m$. In *zz*-exchange spectra, however, such cross-peaks can only be observed if the two spins I_k and I_m possess a common coupling partner I_l. The observation of cross-relaxation is therefore restricted to processes that occur within a network of coupled spins.

We may note that the relevant cross-peaks appear at the frequency coordinates $(\omega_1,\omega_2) = (\Omega_k,\Omega_m)$ in spite of $J_{km} = 0$, which is reminiscent of homonuclear relayed magnetization transfer experiments.[17] In *zz*-exchange spectroscopy, however, the transfer is due to incoherent processes in contrast to the relayed transfer experiment.

Figure 4 shows three strips taken from 2D spectra of the protein basic pancreatic trypsin inhibitor (BPTI), recorded with the experimental scheme of Figure 1a. Parts a and b of Figure 4 show two *zz*-exchange spectra obtained with $\tau_m = 80$ ms and $\tau_m = 200$ ms, while Figure 4c shows a NOESY spectrum with $\tau_m = 200$ ms obtained from the same data set as Figure 4b, by subtracting rather than adding signals obtained with and without π pulse at the beginning of the τ_m period.

The cross- and diagonal-peaks of Ile-18 and of the aromatic protons of Tyr-35 are indicated in Figure 4 (assignments from ref[19]). The amide, C^α and C^β protons of Ile-18 can be identified with the spins I_k, I_l, and I_m, respectively. In the *zz*-exchange spectrum obtained with a short mixing time ($\tau_m = 80$ ms, Figure 4a), only cross-peaks associated with resolved scalar couplings are observed, in agreement with the scheme of Figure 3a. Thus one finds a cross-peak between NH and $C^\alpha H$ of Ile-18, just as in a COSY spectrum. In the *zz*-exchange spectrum obtained with $\tau_m = 200$ ms (Figure 4b), one recognizes an additional cross-peak between NH and $C^\beta H$ at $\omega_1 = 1.86$ ppm. This cross-peak, which has an antiphase doublet structure in both dimensions, arises from the migration

$$2I_{lz}I_{mz} = 2I_z(C^\alpha H)I_z(C^\beta H) \rightarrow 2I_{kz}I_{lz} = 2I_z(NH)I_z(C^\alpha H) \quad (16)$$

and the amplitude is proportional to the cross-relaxation rate constant W_0^{mk} between $C^\beta H$ and NH.

Figure 5 shows three sections parallel to ω_1 taken from the three spectra of Figure 4 at $\omega_2 = 8.13$ ppm, i.e., at the high-frequency component of the NH doublet of Ile-18. The intensity of the *zz* cross-peak at $\omega_1 = 1.86$ ppm, relative to the diagonal peaks at $\omega_1 = 8.11$ ppm in Figure 5b, is ca. 13%, which is comparable to the corresponding ratio in the NOESY spectrum of Figure 5c.

Exchange and Cross-Relaxation in Systems with Four or More Spins

Consider a system with a slow molecular rearrangement which transfers a fragment containing at least two coupled spins between two nonequivalent sites A and B. The spins in a site A will be referred to as I_k and I_l and those in site B as I_m and I_n. Provided that the only nonvanishing couplings are those within the two sites ($J_{kl} \neq 0$, $J_{mn} \neq 0$), and provided that the chemical shift of at least one spin is characteristic of one of the sites, the migration of longitudinal two-spin order $2I_{kz}I_{lz} \rightarrow 2I_{mz}I_{nz}$ can be measured with the experimental schemes of Figure 1.

The initial rate solution of the master equation for pure cross-relaxation in macromolecules (where $W_0 \gg W_1, W_2$) leads to the following coefficients in eq 5:

$$a_{kl,kl}(\tau_m) = 1 - (W_0^{ml} + W_0^{km})\tau_m \quad (17)$$

$$a_{km,kl}(\tau_m) = W_0^{ml}\tau_m$$

$$a_{ml,kl}(\tau_m) = W_0^{km}\tau_m$$

$$a_{mn,kl}(\tau_m) = 0$$

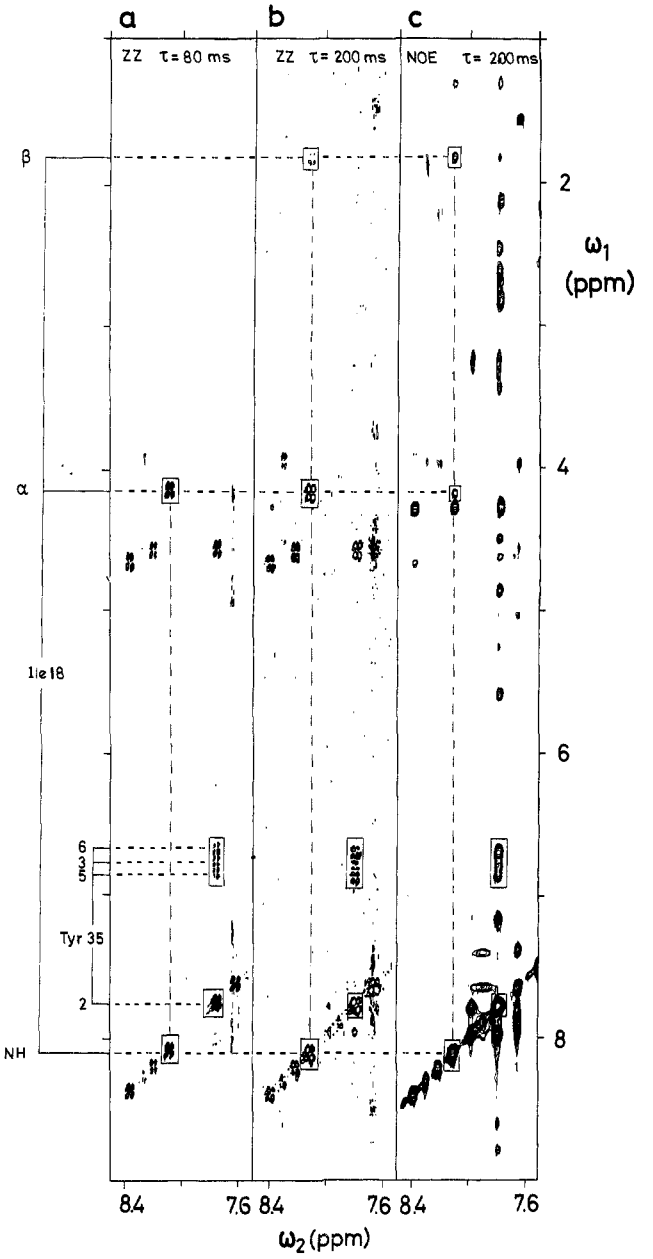

Figure 4. Phase-sensitive 360-MHz spectra of a 20 mM solution of BPTI in ^2H_2O, p^2H 4.6, 36 °C, internal reference TSP, recorded with the pulse sequence of Figure 1a. Only a small part of the spectrum is shown, containing all the signals along ω_1 connected with the amide proton of Ile-18. Both positive and negative levels are shown: (a) *zz*-spectrum recorded with $\tau_m = 80$ ms, (b) *zz*-spectrum recorded with $\tau_m = 200$ ms, and (c) NOESY spectrum with $\tau_m = 200$ ms, obtained from the same data set as in (b) (see text). The flip angles were $\beta = \pi/4$ (4 μs). 512 increments were recorded in t_1 with time-proportional phase incrementation[11,18] for a total spectral width of 6024 Hz with quadrature detection in ω_2. The t_2 domain was extended from 2 to 4 K by zero-filling the t_1 domain from 0.5 to 2 K. Shifted sine-bell windows were applied in both dimensions. For each t_1 value 80 scans were coadded with phase-cycling for pure 2D absorption peakshapes.[11,18] The π pulse in the τ_m interval was shifted systematically to suppress zero-quantum artefacts.[13] (a) Shows only diagonal peaks and direct (NH, $C^\alpha H$) "COSY-type" cross-peaks due to resolved couplings. In spectrum b, one recognizes in addition a (NH, $C^\beta H$) cross-peak with an antiphase structure. The NOESY spectrum c contains a further cross-peak to the C^α-proton of the neighboring spin system Arg-17 at 4.31 ppm. The exchange cross-peaks due to the flipping ring of Tyr-35 (see Figure 6) are also identified.

For longer mixing times, where the initial rate condition is no longer valid, one obtains for pure cross-relaxation in macromolecules the approximate expression

$$a_{mn,kl}(\tau_m) \simeq (W_0^{km}W_0^{nl} + W_0^{kn}W_0^{lm})\tau_m^2 \quad (18)$$

(17) Eich, G. W.; Bodenhausen, G.; Ernst, R. R. *J. Am. Chem. Soc.* **1982**, *104*, 3731–3732.
(18) Marion, D.; Wüthrich, K. *Biochem. Biophys. Res. Commun.* **1983**, *113*, 967–974.
(19) Wagner, G.; Wüthrich, K. *J. Mol. Biol.* **1982**, *155*, 347–366.

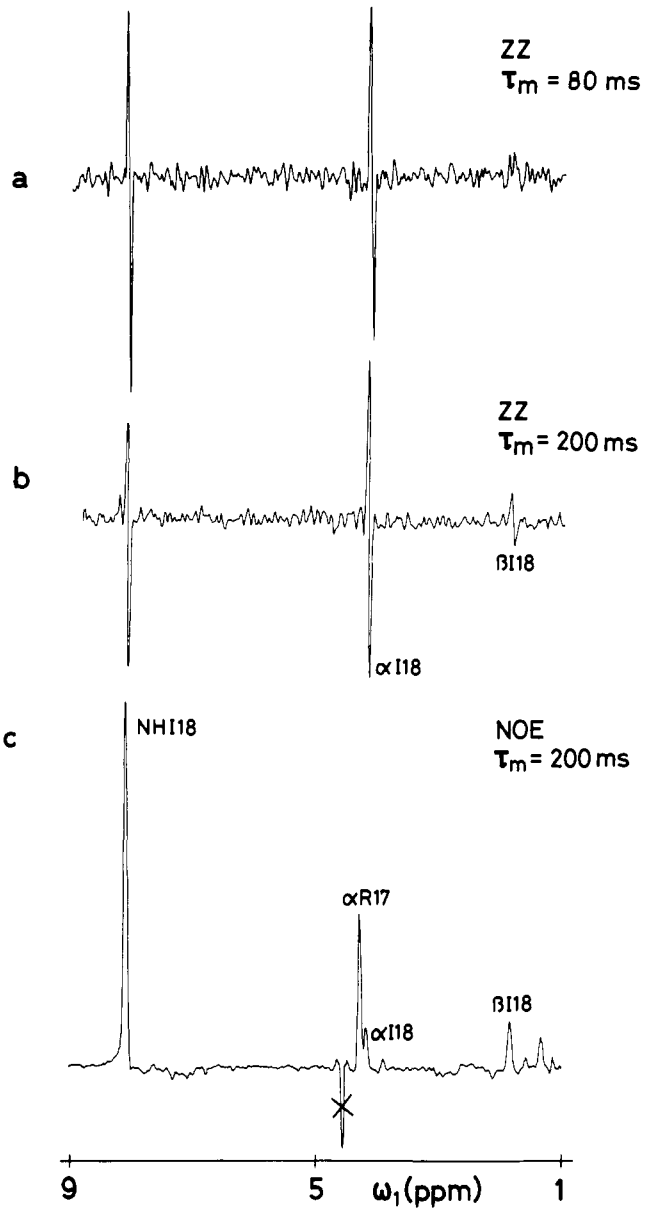

Figure 5. Sections taken parallel to the ω_1 axis from the three spectra in Figure 4 at the ω_2 position of the low-field doublet component of the Ile-18 amide proton. The cross (×) identifies a (negative) tail of the water signal in (c).

On the other hand, a concerted motion of the spins I_k and I_l to the sites of spins I_m and I_n leads to a contribution to the cross-peak amplitudes that is linear with respect to τ_m (assuming a first-order reaction and neglecting spin–lattice relaxation). Thus the combined effect of cross-relaxation and exchange leads to amplitudes

$$a_{mn,kl}(\tau_m) = 2K_{BA}\tau_m + (W_0^{km}W_0^{nl} + W_0^{kn}W_0^{lm})\tau_m^2 \quad (19)$$

For $W_0\tau_m < 2K_{BA}\tau_m$, the amplitude of the cross-peak is directly proportional to the exchange rate, and the effect of cross-relaxation can be readily identified through the quadratic dependence on τ_m (vanishing derivative for $\tau_m = 0$).

By way of example, consider the ring-flip motion of a tyrosine ring embedded within a globular protein, shown schematically in Figure 6a. If the ring-flip motion is slow, the chemical shifts of the four aromatic protons are usually well-resolved, since the environment of the ring in a protein is inherently asymmetric. This situation applies to Tyr-35 in BPTI, where the flip rate is approximately 30 s^{-1} at 309 K[20]. We make the identifications I_k

(20) Wagner, G.; DeMarco, A.; Wüthrich, K. *Biophys. Struct. Mech.* **1976**, *2*, 139–158.

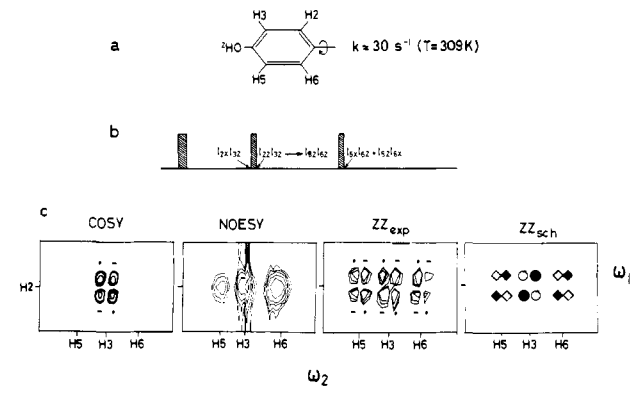

Figure 6. (a) All four aromatic protons of tyrosine rings in proteins generally have different chemical shifts, unless the influence of the asymmetric environment is averaged out by rapid ring-flip motions.[20] (b) Transformation of zz-order if the ring flips in the course of the mixing interval. Only terms derived from $I_{2x}I_{3z}$ are shown here, which lead to signals with $\omega_1 = \Omega_{H2}$. (c) Cross-peaks in COSY, NOESY, and experimental and schematic zz-spectra (τ_m = 200 ms), as discussed in text.

→ H2, I_l → H3, I_m → H5, and I_n → H6. The chemical shifts of these protons are indicated on the left side of Figure 4a. Note that the scalar couplings across the ring are vanishingly small: a COSY spectrum shows only cross-peaks between the protons H2 and H3 and between H5 and H6. By contrast, the zz-exchange spectra of Figure 4a,b shows additional cross-peaks due to the ring-flip motion.

The scheme in Figure 6b shows how additional signals can make their appearance in zz-spectra in the presence of exchange. If we focus attention on the term $I_{2x}I_{3z}$ at the end of the evolution period (which is modulated by the shift Ω_{H2} in t_1 and therefore leads to signals at $\omega_1 = \Omega_{H2}$), the first β-pulse generates two-spin order $I_{2z}I_{3z}$, which in the absence of exchange can only be reconverted into $I_{2z}I_{3z}$ or $I_{2z}I_{3x}$ by the last β pulse, leading to signals at $\omega_2 = \Omega_{H2}$ and Ω_{H3}, respectively (diagonal or COSY-like cross-peaks in zz-exchange spectra). The ring flip, however, may convert $I_{2z}I_{3z}$ into $I_{5z}I_{6z}$ (wavy arrow in Figure 6b), which is transformed by the last β pulse into the terms $I_{5x}I_{6z}$ and $I_{5z}I_{6x}$, leading to signals at $\omega_2 = \Omega_{H5}$ and Ω_{H6}, respectively. The experimental zz-signals are shown in more detail in Figure 6c. All three multiplets have antiphase structure. By contrast, the NOESY cross-peaks in Figure 6c have an in-phase multiplet structure, and the individual multiplet components collapse to broad peaks. (The central peak in the NOESY spectrum in Figure 6c is also distorted by t_1 noise.) The amplitudes in the conventional NOESY spectrum reflect a superposition of exchange and cross-relaxation:

$$a_{n,k}(\tau_m) = (2K_{BA} + W_0^{kn})\tau_m \quad (20)$$

$$a_{m,k}(\tau_m) = W_0^{km}\tau_m$$

$$a_{n,l}(\tau_m) = W_0^{ln}\tau_m$$

$$a_{m,l}(\tau_m) = (2K_{BA} + W_0^{lm})\tau_m$$

Thus in the NOESY spectrum, exchange and cross-relaxation cannot be separated, except possibly by studying the temperature or magnetic field dependence. By contrast, the zz peaks between $\omega_1 = \Omega_{H2}$ and $\omega_2 = \Omega_{H5}$ and Ω_{H6} in Figure 6c can be unambiguously assigned to pure exchange, provided that one verified that the peak intensities increase linearly with τ_m.

Two-dimensional zz-exchange spectroscopy can also be useful in situations where cross-relaxation can be excluded a priori, and where exchange is known to be the mechanism of magnetization transfer. In this case, zz-spectra have the advantage over conventional 2D exchange spectra that at least some cross-peaks are less likely to overlap. In conventional 2D exchange spectra, cross-peaks due to exchange of a particular spin from one environment to another tend to occur fairly close to the diagonal, because the change in chemical shift is in practice often fairly small. Since the vicinity of the diagonal tends to be crowded and

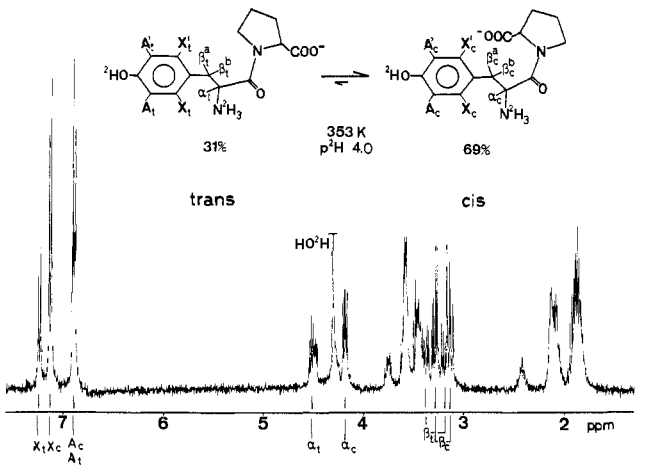

Figure 7. Conformational equilibrium of cis and trans tyrosyl-proline and 360-MHz spectrum with TSP as reference. Because the ring-flip motion is rapid in this case, the protons A_t and A'_t, X_t and X'_t, A_c and A'_c, X_c and X'_c have pairwise identical chemical shifts (two AA'XX' systems, where the shifts of A_c and A_t are accidentally degenerate.)

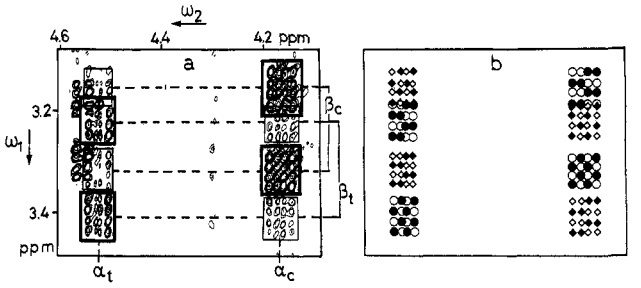

Figure 8. Details of experimental and schematic *zz* spectra of the $C^{\alpha}H$–$C^{\beta}H$ cross-peak region of the cis/trans equilibrium of Figure 7. The parameters were the same as in Figures 4 and 5, except that $T = 80$ °C and $\tau_m = 800$ ms, and a simplified zero-quantum suppression scheme was used, requiring only 16 scans for each t_1 value. Open and filled symbols indicate positive and negative multiplet components, respectively. Peaks due to exchange are represented by diamonds and those due to scalar couplings by circles (COSY-type peaks). The two types are framed in light and heavy lines, respectively. The cross-peaks that are not enclosed in a frame are due to a decomposition product which appeared in the course of the experiment.

susceptible to base line distortions, this may prevent identification of cross-peaks due to exchange. By contrast, exchange cross-peaks in *zz*-spectra may occur at all intersections of the chemical shifts of spin system A with those of system B. This gives rise to a larger number of exchange cross-peaks, many of which may lie far from the diagonal and can thus be easily identified.

We illustrate this feature of *zz*-spectroscopy for the conformational equilibrium of the dipeptide L-tyrosyl-L-proline. The 1D spectrum in Figure 7 shows that the cis and trans forms coexist in dynamic chemical equilibrium.[21] The partial contour map of the *zz*-exchange spectrum in Figure 8 shows a small region containing the cross-peaks between the C^{α} and C^{β} protons of the tyrosyl residues in the two conformers. This region lies far from the diagonal. Cross-peaks which also appear in COSY spectra are identified with heavy frames, those due to the migration of *zz*-order are outlined by light frames. The latter appear at locations which do not carry any signals in NOESY spectra. In the schematic spectrum of Figure 8b, COSY-like *zz*-signals are marked by circles and exchange-type *zz*-signals by diamonds, like in Figure 3. Note that even if the two types of cross-peaks partly overlap, as indeed they do in this stringent test case, it is still possible to measure the amplitudes. The COSY-type and exchange-type *zz*-cross-peaks are located at the corners of a rectangle in the 2D spectrum. The sign patterns of the exchange-type multiplets can be rationalized by noting that the coupling constants

(21) Grathwohl C.; Wüthrich, K. *Biopolymers* **1981**, *20*, 2623–2633.

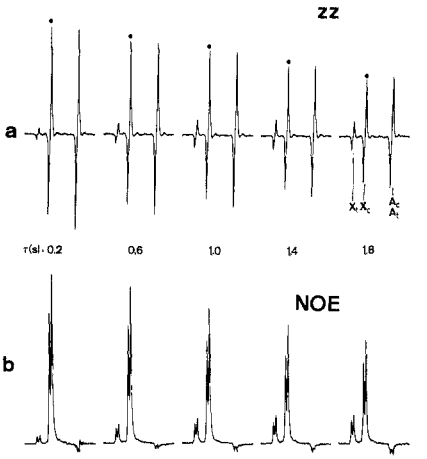

Figure 9. One-dimensional *zz* and NOE difference spectra of the aromatic region of the mixture of cis and trans tyrosyl-proline in dynamic equilibrium (Figure 7), recorded with the scheme of Figure 1b with different mixing times τ_m. The line that was inverted selectively with a pulse of 90 ms duraction is marked with an asterisk. Each spectrum was obtained by linear combination of four scans (see text).

of one conformer are active in the evolution period, while those of the other conformer are relevant in the detection period. If the coupling constants differ before and after exchange, one obtains rectangular antiphase cross-peak patterns, a feature of *zz*-exchange spectra which stands in contrast to the usual square antiphase pattern in COSY spectra.

One-Dimensional *zz*-Exchange Spectroscopy

In spectra with well-separated multiplets which lend themselves to manipulations by selective pulses, similar information can be obtained by the one-dimensional *zz*-method shown schematically in Figure 1b. A selective π pulse applied to a single multiplet component creates longitudinal *p*-spin order. Note that this must be distinguished from conventional transient 1D Overhauser studies, where an entire multiplet must be inverted or saturated. Consider for simplicity a two-spin system, initially in thermal equilibrium, where the effect of a selective π pulse on one of the doublet components of spin I_k can be described by[7]

$$I_{kz} + I_{lz} \xrightarrow{\pi(1/2)(I_{kx} \pm 2I_{kx}I_{lx})} I_{lz} + 2I_{kz}I_{lz} \qquad (21)$$

In the mixing time τ_m, the *z* and *zz* terms migrate as described above for the 2D method. A $\beta = \pi/4$ pulse converts these terms into observable single quantum coherence. To remove signals stemming from transitions that are not affected by these processes, one makes use of difference spectroscopy: a spectrum with the selective pulse set off-resonance is subtracted in alternate scans. Actually, two such difference experiments must be performed, with and without a nonselective π pulse at the beginning of the mixing period, in order to allow one to separate the *z* and *zz* terms by taking the difference or the sum of the two difference spectra, just as in the 2D experiment described above. We may note in parentheses that the *z* subspectrum obtained with $\tau_m = 0$ yields the undistorted multiplet of the irradiated spin I_k, as described recently by Bauer and Freeman,[22] who employed an accurate 90° (composite) monitoring pulse to suppress the effect of *p*-spin order with $p > 1$.

One-dimensional *zz*-spectroscopy is particularly convenient if the migration of *z* or *zz* order must be monitored as a function of the mixing time τ_m (so-called "build-up" plots[23]). To illustrate this feature, 1D *zz*-exchange spectroscopy was applied to study the cis–trans isomerization in L-tyrosyl-L-proline (see 1D spectrum of Figure 7). Note that in contrast to Tyr 35 in BPTI, the rotation

(22) Bauer C.; Freeman, R. *J. Magn. Reson.* **1985**, *61*, 376–381.

(23) (a) Dubs, A.; Wagner, G.; Wüthrich, K. *Biochim. Biophys. Acta* **1979**, *577*, 177–194. (b) Wagner, G.; Wüthrich, K. *J. Magn. Reson.* **1979**, *33*, 675–680. (c) Kumar, Anil; Wagner, G.; Ernst, R. R.; Wüthrich, K. *J. Am. Chem. Soc.* **1981**, *103*, 3654–3658.

of the aromatic ring is fast, and the protons in symmetrical positions on the rings are chemically equivalent (two AA'XX' systems). The high-field component of the X_c doublet of the cis conformer (Figure 7) is inverted selectively, as indicated by asterisks in Figure 9. (Actually, this inversion was not very clean, but nonideal behavior does not prevent one from separating z and zz order by the nonselective π pulse.) The zz order is transferred from the cis to the trans conformer and leads to antiphase doublets at the positions of the A_t and X_t resonances (Figure 7) in the zz-subspectrum. The transfer of z-magnetization leads to in-phase doublets at the same positions in the z-subspectrum. The migration of z-order through cis-trans exchange gives rise to an X_t doublet, while NOE within the cis conformer shows up as a small doublet of opposite sign at the A_c resonance position ($\omega_0\tau_c << 1$ in this system, hence positive NOE in 1D parlance). The increase of both the zz- and z-peaks with τ_m in Figure 9 is approximately linear for short mixing times. While the doublet of X_t increases with τ_m, the high-field signal, which stems from a superposition of the A_t and A_c doublets, shows a decay that is slower than that of the X_c doublet, since the A_c signal decreases while the A_t signal increases like the X_t signal. In the z-subspectrum extracted from the same data (which is equivalent to a conventional transient NOE difference spectrum), the exchange leads to positive X_t signals, while cross-relaxation leads to weak negative A_c signals. In systems where both mechanisms act simultaneously, the buildup of the signals in the zz-subspectrum yields direct information on the exchange rate, in analogy to 2D zz-spectroscopy.

Conclusions

The two examples discussed in this paper, i.e., the slow ring-flip of Tyr-35 in BPTI and the cis-trans isomerization in tyrosyl-proline, serve to illustrate the unique features of 1D and 2D zz-exchange spectroscopy. Future applications will not be restricted to such local molecular rearrangements. There is an abundance of dynamic systems where these methods can provide new insight, such as dynamic equilibria between native and denatured proteins or nucleic acids, between double- and single-stranded DNA fragments, electron exchange in redox-active proteins, chemical exchange in complexes formed between proteins and nucleic acids, or between biopolymers and low molecular weight effector or drug molecules.

Acknowledgment. The authors are indebted for stimulating discussions to Dr. M. H. Levitt. This work was supported in part by the Schweizerischer Nationalfonds (project 3.284.82) and the Kommission zur Förderung der wissenschaftlichen Forschung (projects 1120 and 1329).

Registry No. TyrPro, 51871-47-7; BPTI, 9087-70-1.

Interfacial Electron Transfer in TiO_2 Colloids

Graham T. Brown,[†] James R. Darwent,*[†] and Paul D. I. Fletcher[‡]

Contribution from the Department of Chemistry, Birkbeck College, University of London, London WC1E 7HX, United Kingdom, and the Department of Chemistry, University of Kent, Canterbury CT2 7NZ, United Kingdom. *Received February 15, 1985*

Abstract: Semiconductor colloids can be used to investigate the factors that control interfacial electron transfer. Such reactions are important in the design of new catalysts for photochemical reactions. Previous workers have shown that the surface charge on the particles will control the driving force for electron transfer. In this paper, the change in surface charge with pH is also shown to have a pronounced electrostatic effect on the rate of interfacial electron transfer from colloidal TiO_2 to ionic redox reagents such as methylviologen. The effect can be used to identify the point of zero ζ potential for TiO_2 colloids. The rate of electron transfer also depends on the surface area of the particles, so that larger particles react faster than smaller particles. Since colloids contain a discrete range of particle sizes, the kinetic rate profiles do not show simple monoexponential behavior. Instead the kinetics are characterized by an average rate constant, $\bar{k}_x$, and a parameter, ρ, which describes the spread of the distribution in particle sizes. The origin of this nonmonoexponential behavior was confirmed by applying the same analysis to both the kinetic data and particle size measurements obtained by dynamic laser light scattering for different TiO_2 colloids.

Electrostatic gradients at solid/liquid interfaces can be used to catalyze or direct competing chemical reactions. They are also important in electrochemistry and colloid science. Although semiconductor/liquid junctions have been extensively studied with macroscopic electrodes,[1-3] attention has only recently been focused on the photochemistry of transparent semiconductor colloids. These systems are well suited to time-resolved techniques such as flash photolysis,[4-14] fluorescence,[15-19] and resonance Raman spectroscopy.[20-23] They offer a valuable medium in which to study the parameters that determine interfacial electron transfer.

In colloids containing metal oxide particles, the pH of the solution and the surface area of the particles can control the rate of electron transfer to reagents such as methylviologen (MV^{2+}).[5,6,13,24] In general these colloids will contain particles with a discrete range of surface areas. The larger particles will react faster, so that nonmonoexponential kinetics should be expected. No discussion of this effect has so far appeared in the literature, although a general model for dispersed kinetics in heterogeneous systems was recently developed.[25] We have now

[†] University of London.
[‡] University of Kent. Present address: Department of Chemistry, University of Hull, Hull HU6 7RX, United Kingdom.

(1) Heller, A. *Science (Washington, D.C.)* **1984**, *223*, 1141.
(2) Bard, A. J. *J. Phys. Chem.* **1982**, *86*, 172.
(3) Grätzel, M. *Acc. Chem. Res.* **1981**, *14*, 376.
(4) Henglein, A. *Ber. Bunsen-Ges. Phys. Chem.* **1982**, *86*, 241.
(5) Duonghong, D.; Ramsden, J.; Grätzel, M. *J. Am. Chem. soc.* **1982**, *104*, 2977.
(6) Moser, J.; Grätzel, M. *J. Am. Chem. Soc.* **1983**, *105*, 6547; *Helv. Chim. Acta* **1982**, *65*, 1436; *J. Am. Chem. Soc.* **1984**, *106*, 6557.
(7) Bahnemann, D.; Henglein, A.; Lilie, J.; Spanhel, L. *J. Phys. Chem.* **1984**, *88*, 709.
(8) Bahnemann, D.; Henglein, A.; Spanhel, L. *Discuss. Faraday Soc.* **1984**, *78*.
(9) Kuczynski, J. P.; Milosavljevic, B. H; Thomas, J. K. *J. Phys. Chem.* **1984**, *88*, 980.
(10) Chandrasekaran, K.; Thomas, J. K. *J. Chem. Soc., Faraday Trans. 1* **1984**, *80*, 1163.
(11) Darwent, J. R. *J. Chem. Soc., Faraday Trans. 1* **1984**, *80*, 183.
(12) Brown, G. T.; Darwent, J. R. *J. Chem. Soc., Faraday Trans. 1*, **1984**, *80*, 1631.
(13) Brown, G. T.; Darwent, J. R. *J. Chem. Soc., Chem. Commun.* **1985**, 98.

0002-7863/85/1507-6446$01.50/0